metals

MDPI

Article

Oxidation Kinetics and Oxygen Capacity of Ti-Bearing Blast Furnace Slag under Dynamic Oxidation Conditions

Li Zhang [1,*], Wu Zhang [2], Juhua Zhang [3] and Guangqiang Li [3]

1 School of Materials and Metallurgy, Northeastern University, Shenyang 110819, China
2 School of Materials Science and Engineering, Shenyang Ligong University, Shenyang 110168, China; neusmmzhangwu@163.com
3 The State Key Laboratory of Refractories and Metallurgy, Wuhan University of Science and Technology, Wuhan 430081, China; zhangjuhua@wust.edu.cn (J.Z.); liguangqiang@wust.edu.cn (G.L.)
* Correspondence: zhangl@smm.neu.edu.cn; Tel./Fax: +86-24-8367-0465

Academic Editor: Corby G. Anderson
Received: 23 December 2015; Accepted: 21 April 2016; Published: 6 May 2016

Abstract: The oxidation kinetics of low valence titanium and iron in Ti-bearing blast furnace slag were investigated, the activation energies were calculated, which are 461.1 and 437.3 kJ/mol, respectively. The results illustrate that the oxidation process of Ti^{3+} in the slag is controlled by chemical reactions. However, the chemical reaction between oxygen and iron, between slag and gas, is the determining step of the iron oxidation process. The effects of the isothermal oxidation on the content of Fe_2O_3, Fe_M, FeO, and Fe_T in the slag are discussed. The Fe^{2+} and Ti^{3+} in the molten slag were oxidized at high temperatures. Oxygen affinity of the slag can be described using oxygen capacity. The oxygen capacity of Ti-bearing blast furnace slag was investigated during the dynamic oxidation process, the results indicates that the oxygen capacity of the slag decreased with increasing oxidation time during the dynamic oxidation process.

Keywords: Ti-bearing blast furnace slag; dynamic oxidation; kinetics; oxygen capacity

1. Introduction

China is rich in titanium mineral resources, 95% of the titanium exists in vanadium-titanium magnetite ore [1–3]. During the smelting process of vanadium-titanium magnetite ore, most of the Ti components are concentrated into the slag phase. The TiO_2 content in the slag is about 25 wt. %, moreover, there are 2–6 wt. % metallic iron and 1.4–1.7 wt. % vanadium in the slag. It is estimated that more than three million tons of Ti-bearing blast furnace slag are produced each year in China.

The Ti components in the slag are distributed in various fine grained mineral phases (<10 μm) with complex interfacial combination and this makes it difficult to recover the Ti component through conventional separation processes [1–4]. Several methods have been proposed to separate the titanium components from the slag, such as flotation combined with the magnetic separation method, hydro-metallurgy and the melting reduction method [4–11]. However, all of the aforementioned methods have not been applied in industry due to low recovery or complex process of the methods. Thus, the slag has not been fully used until now.

Perovskite, titanaugite, and Ti-rich diopside are the main titanium-containing mineral phases in the slag [1,7,9]. The valency of titanium is +4, +2, and +3 in perovskite, titanaugite, and Ti-rich diopside phase, respectively. The total content of low valency (Ti^{2+}, Ti^{3+}) titanium constitutes more than 8% which accounts for over 30% of the total titanium oxides in the slag [1,7,9,10]. Several investigations [5–11] showed that low valency of titanium in the molten slag was oxidized to Ti^{4+} and most of the Ti components were enriched into the perovskite phase, and the perovskite phase

grew during the oxidation and cooling process. The perovskite phase, which could be used as raw material in the titanium pigment industry, could be separated from the slag using a mineral dressing method. The obtained tailings can be used as building material. In order to obtain further information on the oxidation of the slag and the crystallization process of the perovskite phase, it was necessary to study the oxidation kinetics of the slag and the effects of dynamic oxidation on crystallization of the perovskite phase.

The dynamic oxidation remarkably influences the viscosity and chemical composition of the molten slag, and these parameters play a key role in selective enrichment, crystallization, and growth of the perovskite phase. The chemistry of oxygen in molten slag is important in dynamic oxidation because the oxygen gas can oxidize the low valency of titanium components during the dynamic oxidation process of the slag. Therefore, it is necessary to investigate the oxygen affinity of the slag. Like the sulfide and phosphate capacity of a slag, the oxygen capacity (O_o) is used to describe the oxygen affinity of the slag in the present work. Higher oxygen capacity (O_o) means that the low valency of titanium can be easily oxidized to (Ti^{4+}) and favors the crystallization of the perovskite.

The purpose of the present work was to focus on the oxidation kinetics and oxygen capacity (O_o) of the molten slag, which could provide crucial information for the extraction of titanium components from the slag.

2. Experimental Details

The slag was provided by Panzhihua Iron and Steel Company (Panzhihua, China). Table 1 shows the main chemical composition of the slag. The slag used in isothermal experiments was milled to 120 μm and dried in an oven at 100 °C for 3 h.

Table 1. Chemical composition of the slag (wt. %).

Chemical Composition (wt. %)										
CaO	SiO_2	TiO_2	Ti_2O_3	FeO	Al_2O_3	MgO	MnO	Fe_M *	S	Others
26.54	24.37	16.90	4.06	1.72	13.76	8.48	0.53	2.50	0.67	0.47

* Fe_M refers to metallic iron.

The slag was heated in a vertical $MoSi_2$ resistance furnace with an R type thermocouple, where the heat treatments were controlled by a program controller. The temperature accuracy was within ±3 °C. The gas flow rate was controlled using a gas flow meter. Compressed air was used as oxidation gas. A lance with an inner diameter of 3 mm was used for blowing air.

In this work, the experimental temperatures were selected from 1390 to 1420 °C. Typically, 200 g of slag was melted in a platinum crucible at high temperatures for 20 min under Ar atmosphere, and then air was blown into the slag with a flow rate of 1 L/min. The blowing time used was 2, 4, 6, 8, 10 and 12 min. Thereafter, the slag was slowly cooled to room temperature with a cooling rate of 5 °C/min. The oxidation time was set to be 2, 4, 6, 8 min during the air flow rate experiments.

FeO, Fe_T (total iron content), Ti_2O_3, and TiO_2 content were measured using quantitative chemical analysis by a titration method. Ti_2O_3 and TiO_2 contents were determined using reduction-oxidation and ammonium ferric sulfate titration methods, respectively. The Ti^{2+} content in the slag was neglected due to its low content in the slag. The FeO content was determined using *o*-phenanthtoline oxidation-reduction, and the Fe_2O_3 content was calculated indirectly from the Fe_T and FeO content.

3. Results and Discussion

3.1. The Effects of the Isothermal Oxidation on the (TiO) and (Ti_2O_3) Content in the Slag

Figure 1 shows the variation of Ti_2O_3 content with the oxidation time at different temperatures.

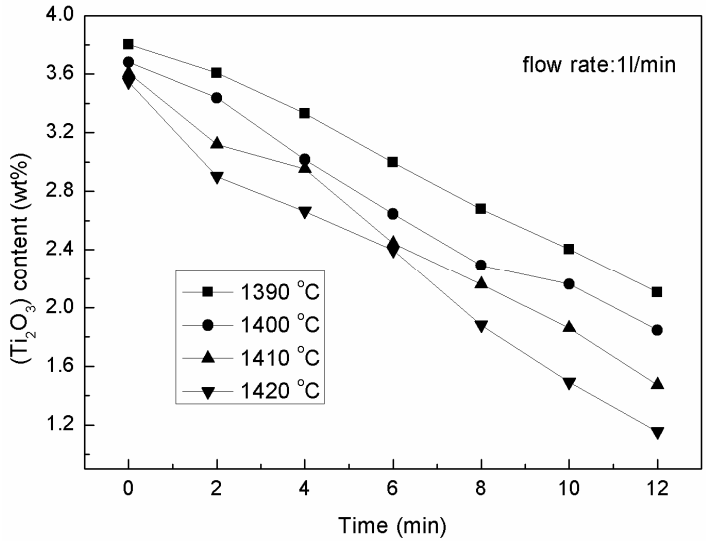

Figure 1. The variation of Ti_2O_3 content at various oxidation times and temperatures.

It is clear that Ti_2O_3 content decreased with the oxidation time and temperature, the oxidation reactions can be represented as [12]:

$$\begin{gathered} \mathrm{TiC\ (s) + O_2\ (g) = (TiO_2) + 0.5CO_2\ (g)} \\ \Delta G^0 = -757,000 + 160.02T\,\mathrm{J/mol}; \\ \Delta G^0_{1693\,\mathrm{K}} = -486,086.14\ \mathrm{J/mol} \end{gathered} \tag{1}$$

$$\begin{gathered} \mathrm{TiN\ (s) + O_2\ (g) = (TiO_2) + 0.5N_2\ (g)} \\ \Delta G^0 = -604,700 + 84.31T\,\mathrm{J/mol}; \\ \Delta G^0_{1693\,\mathrm{K}} = -461,963.17\,\mathrm{J/mol} \end{gathered} \tag{2}$$

$$\begin{gathered} \mathrm{(Ti_2O_3) + 0.5O_2\ (g) = 2\,(TiO_2)} \\ \Delta G^0 = -379900 + 97.04T\,\mathrm{J/mol}; \\ \Delta G^0_{1693\,\mathrm{K}} = -215,611.28\,\mathrm{J/mol} \end{gathered} \tag{3}$$

From the change of Gibbs free energy of the aforementioned reactions, it is obvious that Ti_2O_3, TiN, and TiC in the slag could be easily oxidized under dynamic oxidation conditions.

As mentioned, Ti_2O_3, TiN, and TiC remarkably influence the physical and chemical properties of the slag, such as viscosity and melting point, because TiC and TiN exist in liquid slag in the form of solid particles [1,10–12]. Hence, Ti-bearing slag has a higher viscosity and melting point, and it is to be mentioned that Ti_2O_3 in the molten slag causes an increase of the melting point. After the dynamic oxidation, the Ti_2O_3, TiN, and TiC content were not detectable, which decreased the viscosity and melting point. Table 2 shows the viscosity of the slag at different temperatures.

Table 2. Viscosity of the slag at different temperatures.

Temperature (°C)	Viscosity (Pa· s)
1383	0.331
1373	0.339
1363	0.357
1353	0.379
1343	0.408

3.2. The Effects of the Isothermal Oxidation on the Ferrous Content in the Slag

It has been found that FeO, metallic iron, and Fe_2O_3 are all iron-bearing phases in slag. Low valency iron exists in the form of metallic iron and FeO. During the dynamic oxidation process, low valency iron was oxidized, which can affect the chemical composition and viscosity of the slag. Thus, it can be claimed that dynamic oxidation influences the precipitation and growth of perovskite crystals in the slag.

3.2.1. Variation of the (FeO) Content

Figure 2 shows the variation of FeO content in the molten slag with oxidation time. Figure 3 delineates the variation of FeO content in the molten slag with oxidation time at different air flow rates.

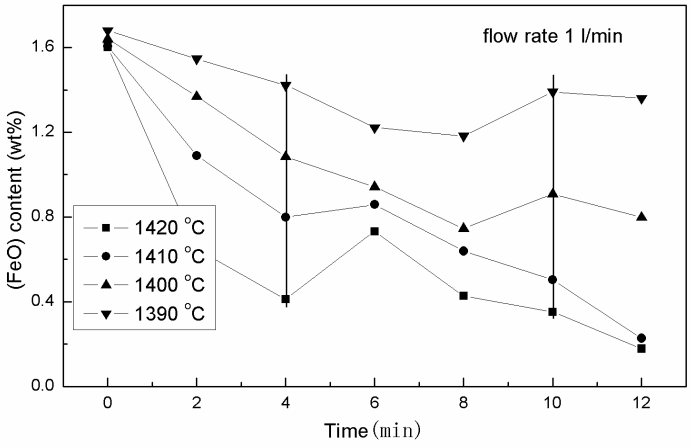

Figure 2. Variation of the FeO content and oxidation time at various temperatures.

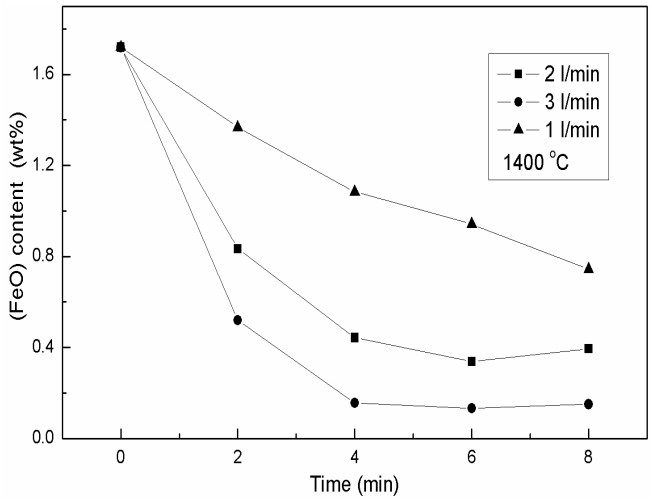

Figure 3. Variation of the FeO content and oxidation time at various flow rates.

As shown in Figure 3, the FeO content decreased in the molten slag with the air flow rate. This means that the oxidation processes of FeO and gas diffusion were accelerated with an increase of oxygen and stirring intensity, which means that increasing the air and stirring intensity can promote the oxidation rate of FeO.

The curves in Figure 2 suggest that the FeO content in the slag changed via the following three stages: In the early stage of oxidation (0–4 min), the oxygen potential increases and FeO is oxidized. Therefore, the FeO content decreases; In the middle stage of oxidation (4–8 min), metallic Fe (in Table 1)

is rapidly oxidized to FeO with an increase in the oxygen potential; In the last oxidation stage (more than 8 min), most of the metallic Fe droplets settled down to the bottom of the crucible and gathered together which makes the metallic Fe content in the slag rapidly decrease (Figure 2), and the oxidation rate of the metallic Fe decreased accordingly.

As shown in Figure 2, the settling rate of the metallic Fe is much greater at 1390 °C and 1400 °C due to the rapid decrease of viscosity at higher temperatures. Moreover, the oxidation rates of FeO at 1410 °C and 1420 °C are much higher than at 1390 °C and 1400 °C; this is the reason why the variation tendency of the FeO content at higher temperatures is more obvious.

The oxygen potential of the slag tends to be low and the FeO content appears to be high. The reaction between FeO and oxygen is [13]:

$$2(\mathrm{FeO}) + 1/2\mathrm{O_2} = (\mathrm{Fe_2O_3}) \quad (4)$$

$$\Delta G^0 = -330,500 + 158T \quad (5)$$

At 1420 °C, the equilibrium constant (K) of Equation (4) can be obtained from Equation (6):

$$K = \exp\left(-\frac{\Delta G^0_{1693}}{RT}\right) = \frac{a_{\mathrm{Fe_2O_3}}}{(a_{\mathrm{FeO}})^2} \times \left(\frac{p}{p^0}\right)^{-1/2} = 78 \quad (6)$$

The value of $\frac{a_{\mathrm{Fe_2O_3}}}{(a_{\mathrm{FeO}})^2}$ obtained via Equation (6) is in the range of 0.78–2.46 as the oxygen potential of the slag in the early stage is lower (10^{-2}–10^{-1} kPa). Obviously, the FeO content would decrease with oxidation time.

The oxidation of TiC, TiN, and Ti(C, N) solid particles around iron beads resulted in a decrease of the viscosity of slag which was beneficial to the aggregation and settlement of the iron droplets. The suspended iron beads in the molten slag are oxidized via the following Equation (7) [12–15]:

$$2\mathrm{Fe\,(l)} + \mathrm{O_2\,(g)} = 2(\mathrm{FeO}) \quad (7)$$

$$\Delta G^0 = -125,860 + 31.92T \quad (8)$$

$$K = \exp\left(\frac{\Delta G^0_{1693}}{RT}\right) = (a_{\mathrm{FeO}})^2 \times \left(\frac{p}{p^0}\right)^{-1} = 164.41 \quad (9)$$

From Equation (8), it is clear that the thermodynamic driving force for Equation (7) is large. However, the oxidation reaction of the iron droplets, which is not homogeneous, involves three phases including gas, liquid, and solid. In fact, only TiC, TiN, and Ti(C, N) on the surface of the iron beads are oxidized in the early oxidation stage. In the middle stage, the FeO content in the molten slag became lower which induced the occurrence of Equation (7). Subsequently, the iron beads began to be oxidized.

3.2.2. Variation of the Fe_M Content

Figure 4 shows the variation of the metallic iron content with the oxidation time at various temperatures, which indicates that the metallic iron content decreases with increased oxidation time and temperature.

Micron-sized Ti(C, N), TiC, and TiN with high specific surface are suspended and dispersed in the molten slag, which can increase the viscosity of the slag. Solids particles, such as TiC and TiN, are usually wrapped around the iron beads surface in the slag to decrease the surface tension, which results in a high metallic iron content in the slag [14].

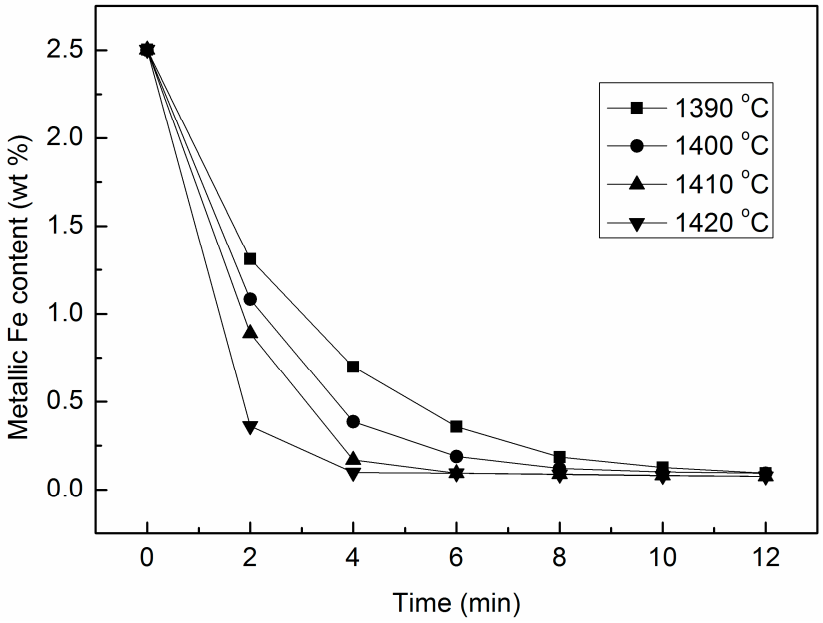

Figure 4. Variation of the metallic iron (MFe) content and oxidation time at various temperatures.

During blowing air to the molten slag, the oxygen potential of the slag increases while the Ti(C, N), TiC, and TiN content as well as the viscosity of the slag rapidly decrease. This makes the suspended iron beads collate, which further reduces the iron content of the slag. An increase in the oxidation temperature accelerates the oxidation and the metallic iron is oxidized and converted into FeO and Fe_2O_3.

3.2.3. Variation of Fe_2O_3 Content

The changes of Fe_2O_3 content in molten slag varying with oxidation time and air flow rate is displayed in Figure 5.

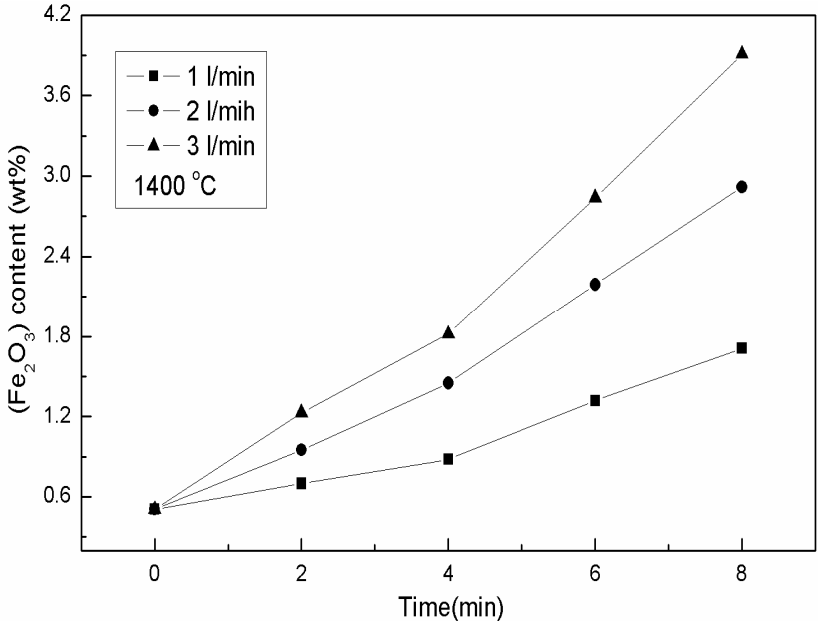

Figure 5. Variation of the Fe_2O_3 content and the time at various flow rates.

As shown in Figure 5, the Fe_2O_3 content increased with the air flow rate, which indicated that FeO and metallic Fe in the molten slag were oxidized. The increase in air flow rate represents an increase of oxygen gas, which resulted in decreasing the viscosity of the liquid slag, and then the settling and oxidation of iron were promoted. Therefore, the Fe_M content in the slag reduced dramatically. On the other hand, increasing the air flow rate improved the stirring intensity and the interfacial reaction between slag and gas phase [16,17]; this accelerates the diffusion of gas to the molten slag and increases the oxidation rate of TiC on the surface of the iron droplets. In general, the Fe_2O_3 content in the slag is indicative of the oxidation state of the slag [13]. When oxygen in the slag is in equilibrium, the Fe_2O_3 content can be regarded as the oxygen potential of the molten slag, thus high oxygen potential means high Fe_2O_3 content.

3.2.4. Variation of the Total Iron Content

Figure 6 displays the variation of total iron content (Fe_T) in the slag with oxidation time. The total iron content (TFe) in this work means the combination of element iron, ferrous oxide (FeO), and ferric oxide (Fe_2O_3).

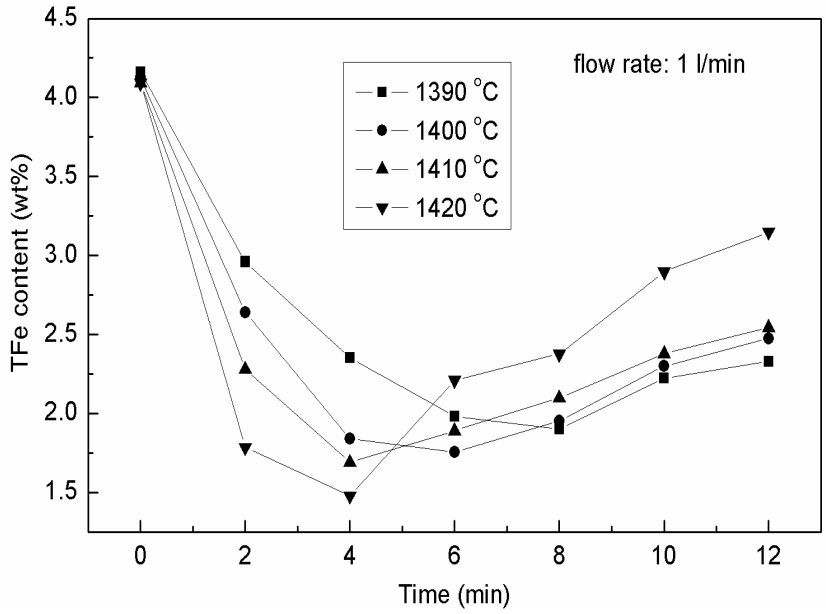

Figure 6. Variation of the total iron content (TFe) content and oxidation time at various temperatures.

In the early oxidation stage, a large quantity of the iron beads were released from TiC particles and precipitated from the molten slag due to the decrease of the slag viscosity and oxidation of TiC particles. Hence, the amount of suspended iron in the slag decreased. The slag viscosity decreases with increasing of temperature. This phenomenon is conducive to the settlement of the iron beads and resulted in a rapid decrease of the metallic Fe content in the slag.

In the final oxidation stage, the suspended iron beads begin to oxidize, the oxidation of metallic iron belongs to a liquid-gas reaction, it was much slower than the oxidation of Fe^{2+}, thus the total iron content (Fe_T) was almost constant at the beginning and then increased gradually.

3.3. Isothermal Oxidation Kinetics of Molten Slag

3.3.1. Oxidation Kinetics of Low Valence Titanium

The oxidation rate of low valency titanium can be described as $\ln[(Ti^{3+})_0/(Ti^{3+})_t]$ where, $(Ti^{3+})_t$ and $(Ti^{3+})_0$ represent the content of Ti^{3+} at time t and zero (initial condition).

Figure 7 shows the variation of the Ti^{3+} content at different air flow rates during the dynamic oxidation process. As shown in Figure 7, the oxidation rate of Ti^{3+} increased with increasing air flow rate, temperature, and oxidation time, and the relation between $\ln[(Ti^{3+})_0/(Ti^{3+})_t]$ and t was linear. Assuming that the chemical reactions are determined by the oxidation rate, the oxidation rate of Ti^{3+} can be represented as:

$$-\frac{dc}{dt} = kc \tag{10}$$

Or:

$$\frac{dc}{dt} = -kc \tag{11}$$

where, c is the concentration of (Ti^{3+}), k is the reaction rate constant.

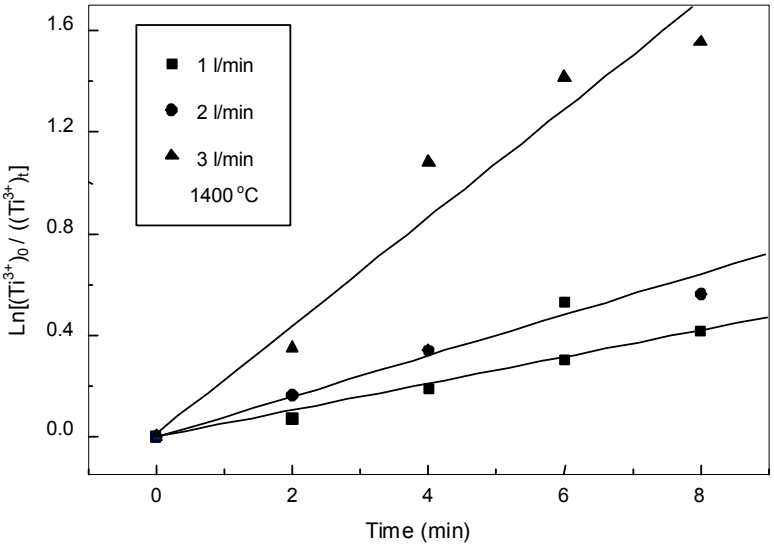

Figure 7. Variation of $\ln[(Ti^{3+})_0/(Ti^{3+})_t]$ and the oxidation time at various flow rates.

Equation (11) can be written as:

$$\ln c = -kt + B \tag{12}$$

where, B is integration constant.

Assuming c_0 is the concentration of a reactant at the starting time, substituting c_0 into Equation (12), B is equal to $\ln C_0$, then the Equation (12) can be changed by:

$$\begin{array}{c} \ln c = -kt + \ln c_0 \\ \text{or } k = (\frac{1}{t}) \times \ln(\frac{c_0}{c}) \end{array} \tag{13}$$

Replacing c_0 and c with $(Ti^{3+})_0$ and $(Ti^{3+})_t$, Equation (13) would be:

$$k = (\frac{1}{t}) \times \ln\left(\frac{(Ti^{3+})_0}{(Ti^{3+})_t}\right) \tag{14}$$

For the first-order reaction, $\ln\left(\frac{(Ti^{3+})_0}{(Ti^{3+})_t}\right)$ is linearly proportional to t where the rate constant represents the slope.

As shown in Figures 7 and 8 the values of $\ln\left(\frac{(Ti^{3+})_0}{(Ti^{3+})_t}\right)$ and time t are plotted which show straight lines, and the oxidation rate of (Ti^{3+}) depends on its concentration and temperature.

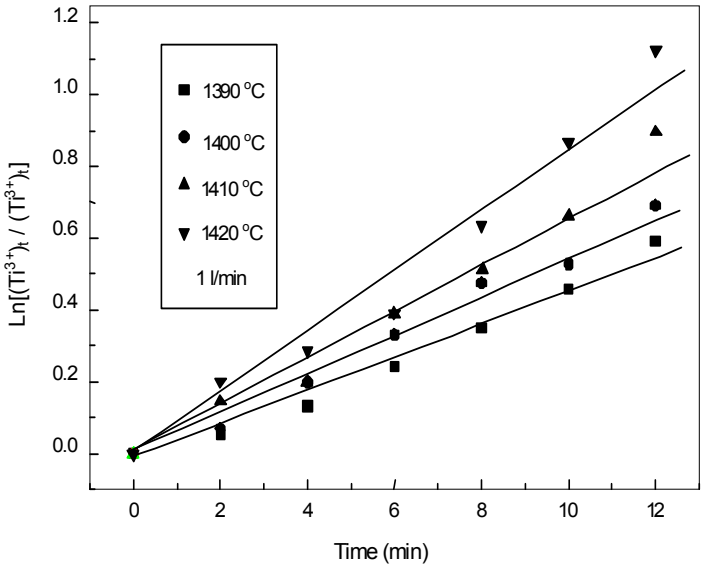

Figure 8. Variation of $\ln[(Ti^{3+})_0/(Ti^{3+})_t]$ and the oxidation time at various temperatures.

The relationships between reaction rate and Ti^{3+} content obey a first order reaction at constant temperature and can be described by the following equation [16]:

$$(Ti^{3+})_t = (Ti^{3+})_0 e^{-kt} \quad (15)$$

The values of the reaction rate constants, which are listed in Tables 3 and 4 are calculated based on the slopes of straight lines in Figures 7 and 8.

Table 3. Rate constant, k_{Ti} at various temperatures.

T/K	k_{Ti}	$-\ln k_{Ti}$
1663	0.0501	2.993734
1673	0.05838	2.840782
1683	0.07203	2.630673
1693	0.09013	2.406502

Table 4. Rate contant, k_{Ti} at different air flow rates.

Air Flow Rate (L/min)	k_{Ti}	$-\ln k_{Ti}$
1	0.05838	2.840182
2	0.07578	2.579921
3	0.18741	1.674437

However, Arrhenius Equation (14) can be expressed as:

$$\frac{d\ln k_{Ti}}{dt} = \frac{E}{RT^2} \quad (16)$$

where, E denotes the activation energy (kJ/mol). Equation (16) can be represented as:

$$\ln k_{Ti} = -\frac{E}{RT} + B \quad (17)$$

The slope of the line in Figure 9 is 4.90.

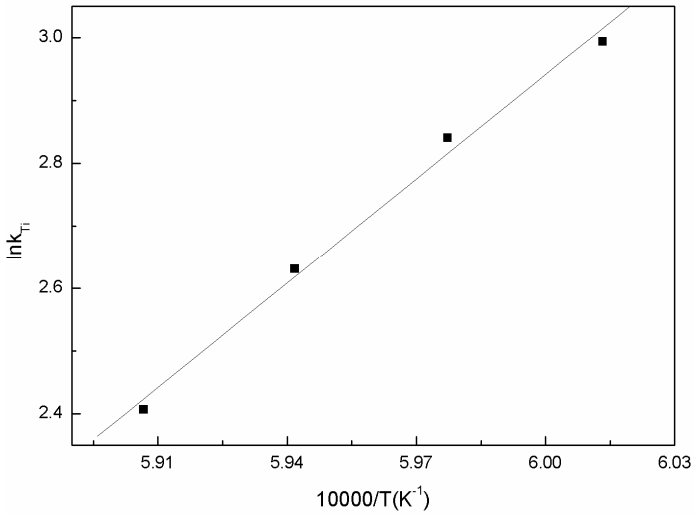

Figure 9. Plot of $\ln k_{\mathrm{Ti}}$ against $1/T$.

Therefore, the activation energy was 461.1 kJ/mol. Thus, Equation (17) can be expressed as:

$$\ln k_{\mathrm{Ti}} = -\frac{55490}{T} - 30.35 \tag{18}$$

When the activation energy was less than 150 kJ/mol, the diffusion process would be the determining step [17]. On the other hand, the reaction would be controlled by an interfacial reaction if the activation energy is larger than 400 kJ/mol [18]. According to the calculated value of the activation energy, it can be deduced that the oxidation process of Ti^{3+} in the slag was controlled by chemical reactions between oxygen and (Ti^{3+}) at the interface between the slag and the gas.

3.3.2. Oxidation Mechanism of Ti^{3+}

Based on the gas-liquid double layer theory, the oxidation process of Ti^{3+} in the slag can be mainly categorized into the following steps [17]:

(1) Oxygen gas arrived at the interface between gas phase (gas film) and the slag phase.

(2) (Ti^{3+}) was oxidized on the interface between slag and gas, thus (Ti^{4+}) was produced via the following reaction:

$$4\left(\mathrm{Ti}^{3+}\right) + \mathrm{O}_{2,(\mathrm{on\ \ interface})} = 4\left(\mathrm{Ti}^{4+}\right) + 2(\mathrm{O}^{2-}) \tag{19}$$

(3) (Ti^{4+}) ions diffused into the molten slag.

Therefore, the oxidation of Ti^{3+} involved mass transfer and chemical reactions. It is generally believed that steps (1) and (2) are faster than (3) and (4) [19–21], but the entire oxidation process was controlled by step (3). The directional migrations of (Ti^{3+}) ions in the slag were determined by the chemical potential gradient.

If diffusion becomes the determining step, the rate equation can be given by the following equations:

$$k_{\mathrm{n}} = \left(\frac{1}{t}\right)\ln\left(\frac{(c_{\mathrm{n}} - c_0)}{(c_{\mathrm{n}} - c_t)}\right) \tag{20}$$

and,

$$Q(c) = \ln\left(\frac{(c_{\mathrm{n}} - c_0)}{(c_{\mathrm{n}} - c_t)}\right) \tag{21}$$

where, c_n is the concentration of (Ti^{3+}) on the interface of the slag and oxygen gas, c_0 and c_t are the concentrations at the initial time and t, respectively; k_n is the diffusion rate constant. A comparison between the results obtained in the present work and the literature is shown in Figure 10.

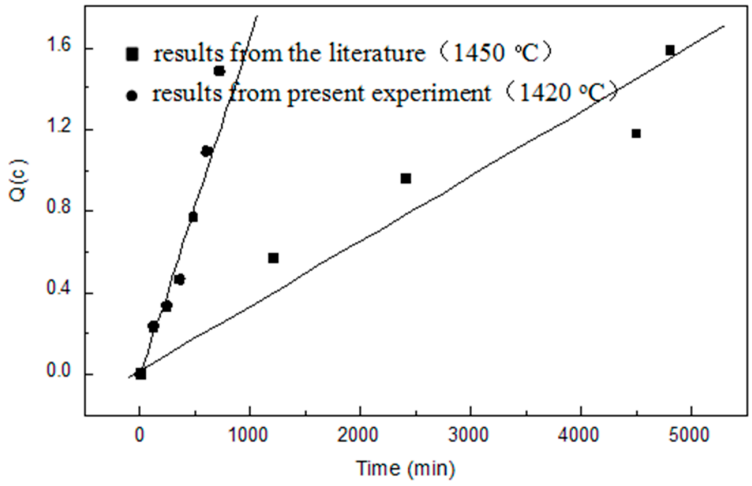

Figure 10. Variation of $Q(c)$ and time in present work and literature (stirring intensity: 15–17 rpm).

The rate constant obtained in the present study (1.56×10^{-4} m·s^{-1}) is much higher than the one (5.8×10^{-6} m·s^{-1}) reported in ref. [1]. The reason for the difference is that the diffusion was promoted by increasing the stirring intensity and introducing air into the molten slag. Hence, in the present work, the oxidation process of Ti^{3+} in the slag was controlled by the chemical reactions.

3.3.3. Oxidation Kinetics of Iron in the Slag

Fe^{2+} is spontaneously oxidized during the oxidation of Ti^{3+}. The oxidation kinetics of iron in the slag can be described by the production rate of (Fe^{3+}). The oxidation reaction is shown in Equation (22).

$$4\left(Fe^{2+}\right) + O_{2,(on \quad interface)} = 2(O^{2-}) + 4\left(Fe^{3+}\right) \tag{22}$$

The oxidation rate equation of iron is identical to that of low valence titanium components. The production rates of Fe^{3+} content with oxidation time and temperature are shown in Figure 11. There is a linear relationship between $\ln\left(\frac{(Fe^{3+})_0}{(Fe^{3+})_t}\right)$ and t. In addition, Fe^{3+} concentration obeys a first order equation [17].

$$(Fe^{3+})_t = (Fe^{3+})_0 e^{-kt} \tag{23}$$

where, $(Fe^{3+})_t$ represents the Fe^{3+} content at time t; $(Fe^{3+})_0$ is the initial concentration.

The slopes of the lines in Figure 11 shows the reaction rate constants at different temperatures, which are listed in Table 5.

Table 5. Rate constant, k_{Fe} at various temperatures.

T/K	k_{Fe}	$-\ln k_{Fe}$
1663	0.10507	2.296901
1673	0.12945	2.044461
1683	0.15741	1.848901
1693	0.17544	1.740458

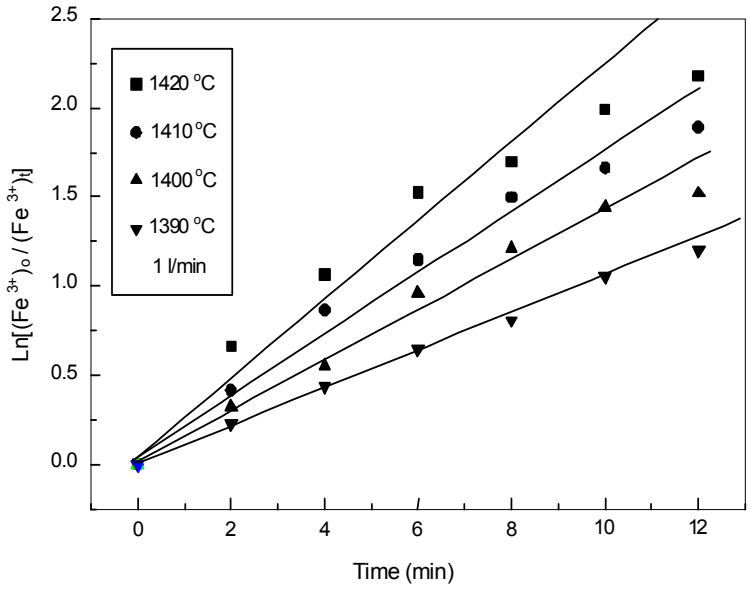

Figure 11. Variation of $\ln[(Fe^{3+})_0/(Fe^{3+})_t]$ and time at various temperatures.

According to the Arrhenius equation [17]:

$$\ln k_{Fe} = -\frac{E}{RT} + B \tag{24}$$

$$\ln k_{Fe} = -\frac{437300}{T} - 29.34 \tag{25}$$

The plotting of $\ln k_{Fe}$ against $1/T$ represents a straight line where $-E/R$ is the slope shown in Figure 12. The calculated activation energy is 437.3 kJ/mol.

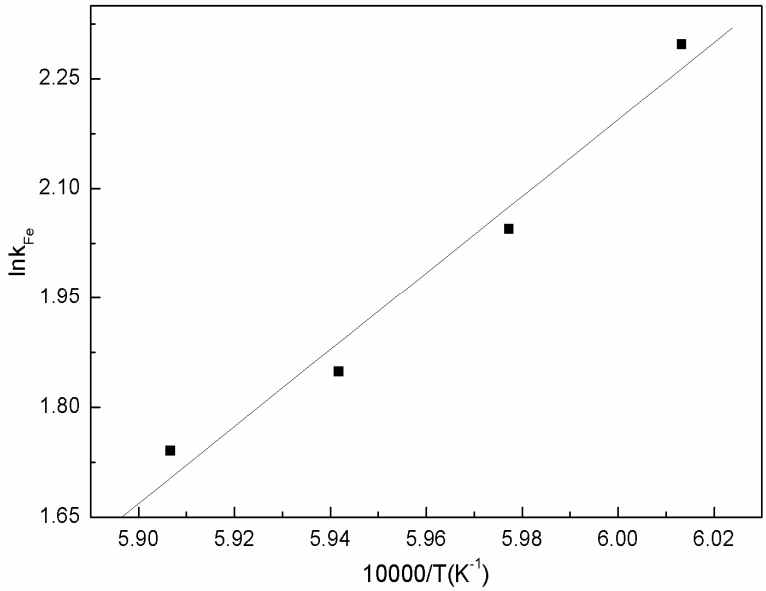

Figure 12. Plot of $\ln k_{Fe}$ against $1/T$.

As mentioned before, it can be confirmed from the value of the activation energy that the chemical reaction between oxygen and iron occurred on the interface of the slag, and gas is the determining step.

The activation energy is close to the rate constants for titanium and iron oxidation, which indicates a coupled reaction occurred between the oxidations of Fe and Ti, which can be represented by the following reaction:

$$(Ti^{3+}) + (Fe^{3+}) = (Fe^{2+}) + (Ti^{4+}) \quad (26)$$

Hence, the oxidation kinetics of Ti^{3+} is equivalent to that of Fe^{3+}.

3.4. Oxygen Capacity of the Slag

The oxidation reactions of iron and titanium components were instantaneous and were locally equilibrium rather than a non-equilibrium state. The ratios of Fe^{3+}/Fe^{2+} and Ti^{4+}/Ti^{3+} changed during the dynamic oxidation process. For the iron and oxygen system, the equilibrium concentration relationships between reactant and product can be represented by:

$$(Fe_2O_3) = 2\,(FeO) + 1/2O_2 \quad (27)$$

$$k = \frac{a^2_{(FeO)}(p/p^0)^{1/2}}{a_{(Fe_2O_3)}} \quad (28)$$

In the metallurgical process of iron and steel making, the ability of the slag to absorb sulfur and phosphorus can be expressed by the sulfide capacity (*C*s) and the phosphate capacity (C_{PO_4}) [15]. During the dynamic oxidation of the slag, the oxygen capacity represents the ability of the slag to absorb oxygen. It is believed that the greater the system deviates from the equilibrium state, the stronger the ability to absorb oxygen.

In the present study, the main oxidation reactions occurring in the molten slag can be represented as:

$$2Fe + 2[O] = 2(FeO) \quad (29)$$

$$4(FeO) + 2[O] = 2(Fe_2O_3) \quad (30)$$

$$4(FeO) + 2[O] = 2(Fe_2O_3) \quad (31)$$

By combining Equations (29)–(31), Equation (32) is obtained:

$$Fe + (FeO) + (Ti_2O_3) + 3[O] = (Fe_2O_3) + 2(TiO) \quad (32)$$

The equilibrium constant of Equation (32) can be expressed as:

$$k = \frac{a_{Fe} \cdot a_{FeO} \cdot a_{Ti_2O_3} \cdot a^3_O}{a_{Fe_2O_3} \cdot a^2_{TiO_2}} \quad (33)$$

The a^3_O in Equation (33) can be expressed as:

$$a^3_O = k\frac{a_{Fe_2O_3} \cdot a^2_{TiO_2}}{a_{FeO} \cdot a_{Fe} \cdot a_{Ti_2O_3}} \quad (34)$$

Thus the oxygen capacity (O_o) of the slag can be defined as:

$$O_o = \frac{(a_{FeO}) \times (a_{Ti_2O_3}) \times (a_{Fe})}{(a_{Fe_2O_3}) \times (a_{TiO_2})^2} \quad (35)$$

$$O_o = \frac{(\gamma_{FeO} \cdot x_{FeO}) \times (\gamma_{Ti_2O_3} \cdot x_{Ti_2O_3}) \times (\gamma_{Fe} \cdot x_{Fe})}{(\gamma_{Fe_2O_3} \cdot x_{Fe_2O_3}) \times (\gamma_{TiO_2} \cdot x_{TiO_2})^2} \quad (36)$$

It was reported in [15–21] that the activity coefficients of FeO_x and TiO_x in slag can be considered as constant when the basicity and the content of the other components are relatively constant. Hence, the ratio of $\gamma_{Ti_2O_3}/\gamma_{TiO_2}$, $\gamma_{FeO}/\gamma_{Fe_2O_3}$ can be considered to be constant. However, by substituting the mole fractions of the concerned substance such as, $a_{Fe} = 1$ ($Fe_{(S)}$ Solid phase pure substance) into Equation (37), the oxygen capacity can be obtained at various oxidation temperature and times. The variation of the oxygen capacity is shown in Figure 13.

$$O_o = \frac{x_{FeO}}{x_{Fe_2O_3}} \cdot \frac{x_{Ti_2O_3}}{x_{TiO_2}} \tag{37}$$

where, x_{FeO} is the activity coefficient of FeO. It is evident that the oxygen capacity of the slag decreases with increasing oxidation time and temperature (Figure 13). This means, the reducing substance decreases with increasing oxidation time and temperature. However, the oxygen capacity of the slag remains constant when the system eventually reaches equilibrium.

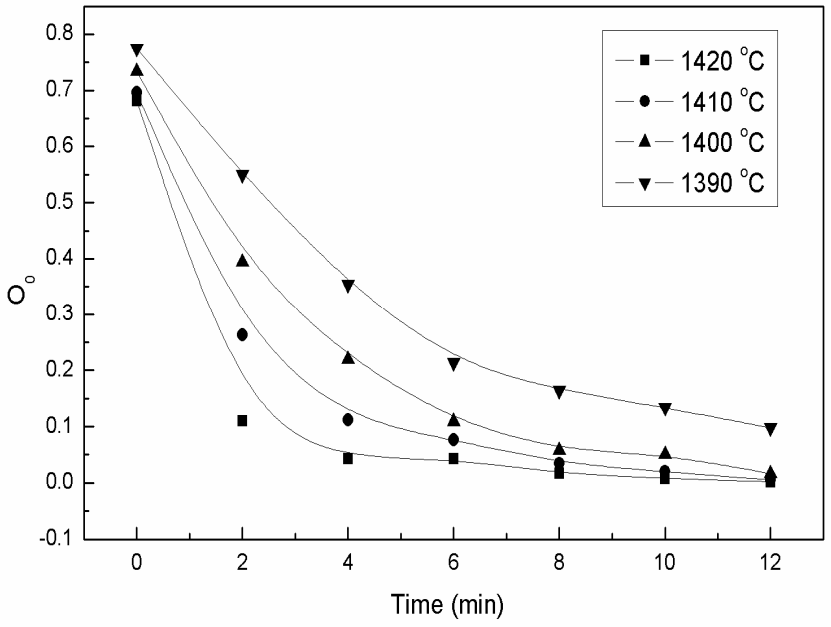

Figure 13. Variation of the oxygen capacity against time.

Figure 14 shows the variation ratio of $x_{TiO_2}/x_{TiO_{1.5}}$ and $x_{FeO_{1.5}}/x_{FeO}$ at 1420 °C. As shown, the change in the relative contents of various ions, such as iron ions and titanium ions in slag is co-ordinated the same. Overall, the slag system is not in equilibrium and the ratio of Fe^{3+}/Fe^{2+} changes with increasing oxidation temperature for low valence titanium and iron.

Comparing Figure 13 with Figure 14, it can be found that the oxygen potential and oxygen capacity were increased and decreased with increasing oxidation temperature and time, which indicated that it would be more difficult for the slag to be oxidized continuously as the oxidizing capacity of the slag increases.

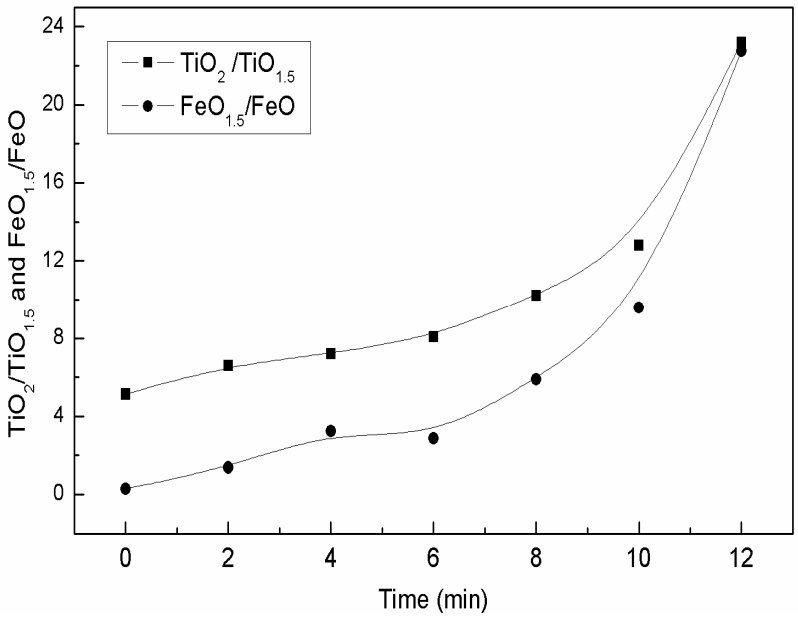

Figure 14. Plot of $x_{TiO_2}/x_{TiO_{1.5}}$ and $x_{FeO_{1.5}}/x_{FeO}$ against time at 1420 °C.

4. Conclusions

The oxidation reaction of low valency titanium components, metallic iron, and Fe^{2+} in molten slag were studied during the dynamic oxidation process. Ferrous components were oxidized at high temperatures during oxidation of the molten slag. Oxidation of Fe^{2+} and Ti^{3+}, which were the kinetically controlling steps, occurred on the interface between gas and slag. The oxidation kinetics equations were established by Ti^{3+} oxidation and Fe^{3+} formation. The oxygen affinity of the slag can be described by the oxygen capacity, and the greater the oxygen capacity (O_o) the stronger the ability of the slag to absorb oxygen.

Acknowledgments: The authors gratefully acknowledge the financial support from Open Research Fund of Key Laboratory for Ferrous Metallurgy and Resources Utilization of Ministry of Education, Wuhan University of Science and Technology, P. R. China NO. FMRU2007K10.

Author Contributions: Li Zhang and Guangqiang Li conceived and designed the study, and they reviewed and edited the manuscript. Wu Zhang and Juhua Zhang performed the experiments. Wu Zhang wrote the paper. All authors read and approved the manuscript.

Conflicts of Interest: The authors declare no conflict of interest.

References

1. Zhang, L.; Zhang, L.N.; Wang, M.Y.; Li, G.Q.; Sui, Z.T. Recovery of titanium compounds from molten Ti-bearing blast furnace slag under the dynamic oxidation condition. *Miner. Eng.* **2007**, *20*, 684–693. [CrossRef]
2. Wang, M.Y.; Zhang, L. Selective enrichment of TiO_2 and precipitation behavior of perovskite phase. *Trans. Nonferrous Met. Soc.* **2006**, *16*, 421–425. [CrossRef]
3. Li, J.; Wang, X.D.; Zhang, Z.T. Crystallization behavior of rutile in the synthesized Ti-bearing blast burnace slag using single hot thermocouple technique. *ISIJ Int.* **2011**, *51*, 1396–1402. [CrossRef]
4. Zhang, L.; Li, G.Q.; Lou, T.P.; Sui, Z.T. Selective enrichment and growth of Ti component in titaniferrous slag. *Acta Metall. Sin.* **2002**, *38*, 400–403.
5. Sui, Z.T. Precipitation selectivity of boron components from slags. *Acta Mater.* **1999**, *47*, 1337–1344. [CrossRef]
6. Zhang, L.; Zhang, J.H.; Zhang, W.; Li, G.Q. Thermodynamic analysis of extraction of synthetic rutile from modified slag. *Ind. Eng. Chem. Res.* **2013**, *52*, 4924–4931. [CrossRef]

7. Zhang, L.; Zhang, L.N.; Wang, M.Y. Effect of perovskite phase precipitation on viscosity of Ti-bearing blast furnace slag under the dynamic oxidation condition. *J. Non Cryst. Solids* **2006**, *352*, 123–129. [CrossRef]
8. Zhang, L.; Zhang, L.N.; Sui, Z.T. Dynamic oxidation of the Ti-bearing blast furnace slag. *ISIJ Int.* **2006**, *46*, 458–465. [CrossRef]
9. Zhang, L.; Zhang, L.N.; Wang, M.Y. Precipitation selectivity of perovskite phase from Ti-bearing blast furnace slag under the dynamic oxidation condition. *J. Non-Cryst. Solids* **2007**, *353*, 2214–2290. [CrossRef]
10. Zhang, W.; Zhang, L.; Zhang, J.H.; Feng, N.X. Crystallization and coarsening kinetics of rutile phase in modified Ti-bearing blast furnace slag. *Ind. Eng. Chem. Res.* **2012**, *51*, 12294–12298.
11. Zhang, W.; Zhang, L.; Zhang, J.H.; Feng, N.X. Effect of oxidation on phase transformation in Ti-bearing blast furnace slag. *Adv. Mater. Res.* **2013**, *641*, 363–366. [CrossRef]
12. Wang, X.D.; Mao, Y.W.; Liu, X.Y.; Zhu, Y.K. Study on crystallization behavior of blast furnace slag containing TiO_2. *J. Iron Steel Res.* **1990**, *3*, 1–6.
13. Li, Y.H.; Lou, T.P.; Sui, Z.T. Kinetics of non-isothermal precipitate process of perovskite phase in CaO-TiO_2-SiO_2-Al_2O_3-MgO system. *J. Mater. Sci.* **2000**, *35*, 5635–5637. [CrossRef]
14. Pistourious, P.C.; Coetzee, C. Physicochemical aspects of titanium slag production and solidification. *Metall. Mater. Trans. B* **2003**, *34*, 581–586. [CrossRef]
15. Lou, Y.P.; Li, Y.H.; Sui, Z.T. Study of precipitation of perovskite phase from the oxide slag. *Acta Metall. Sin.* **2000**, *36*, 140–144.
16. Xue, X.X.; Duan, P.N.; Zhou, M. Review of thermodynamic studies on titanium oxides in metallurgical slags. *J. Baotou Univ. Iron Steel Technol.* **1999**, *18*, 357–362.
17. Li, J.; Zhang, Z.T.; Zhang, M.; Guo, M.; Wang, X.D. The influence of SiO_2 on the extraction of Ti element from Ti-bearing blast furnace slag. *Steel Res. Int.* **2011**, *82*, 613–614. [CrossRef]
18. Li, D.G.; Wang, J.F.; Lou, T.P.; Sui, Z.T. Precipitation kinetics of calcium cerite phase in slag bearing rare earths. *J. Iron Steel Res.* **2004**, *16*, 64–67.
19. Liu, X.H.; Sui, Z.T. Leaching of Ti-bearing blast furnace slag by pressuring. *Trans. Nonferrous Met. Soc.* **2002**, *12*, 1281–1284.
20. Li, L.S.; Sui, Z.T. Physical chemistry behavior of enrichment the selectivity of TiO_2 in perovskite. *Acta Phys. Chem. Sin.* **2001**, *17*, 845–849.
21. Xia, Y.H.; Sui, Z.T. Computer simulation of phase separation in CaO-MgO-Fe_2O_3-Al_2O_3-SiO_2 glass. *J. Northeast. Univ.* **1999**, *5*, 511–514.